ELSEVIER

International Journal of Mass Spectrometry 212 (2001) 491–504

International Journal of Mass Spectrometry

www.elsevier.com/locate/ijms

Inelastic ion-surface collisions: scattering and dissociation of low energy benzene molecular cations

Helen L. de Clercq[a,b], Atish D. Sen[a,c], Anil K. Shukla[a,d,*], Jean H. Futrell[a,d,*]

[a]*Department of Chemistry and Biochemistry, University of Delaware, Newark, Delaware 19716*
[b]*Howard University, Department of Chemistry, Washington, District of Columbia 20059*
[c]*Du Pont Marshall Laboratory, Philadelphia, Pennsylvania 19104*
[d]*Environmental Molecular Sciences Laboratory, Pacific Northwest National Laboratory, P.O. Box 999, Richland, Washington 99352*

Received 24 May 2001; accepted 30 July 2001

Abstract

We have studied collisions of benzene cations with a self-assembled monolayer surface of alkanethiol on gold substrate at kinetic energies ranging from 10 to 50 eV at 45° impact angle using a modified crossed-beam tandem mass spectrometer. Neutralization is the main reaction at all kinetic energies investigated. At ion kinetic energies below 10 eV, most reflected benzene cations are inelastically scattered with little fragmentation even though they lose most of their kinetic energy in the collision process. As ion energy is increased, the probability of surface-induced dissociation (SID) increases rather slowly. At all energies investigated neither elastic scattering nor SID occurs at the specular scattering angle. The total energy lost by benzene ions in inelastic/dissociative collisions increases as the ion kinetic energy is increased. Kinetic energy distributions of inelastically scattered benzene ions are rather broad and strongly dependent upon the ion kinetic energy. At lower energies, there is only one peak in the kinetic energy distribution of inelastically scattered benzene ions whereas at 50 eV benzene ions exhibit three peaks distinguishable in both energy and scattering angle. The high-energy peak corresponds to nearly zero energy loss (quasielastic scattering) and the lowest energy peak is quasithermalized. These two peaks are narrower than the central main peak suggesting a different dynamic mechanism for each of these collision processes. (Int J Mass Spectrom 212 (2001) 491–504) © 2001 Elsevier Science B.V.

Keywords: Ion-surface collisions; Surface-induced dissociation; Scattering; Energy transfer; Kinetic energy distributions

1. Introduction

The interaction of ions with metal surfaces has been a subject of intensive research in the physics community for some time [1–7]. This research is motivated, in part, by the desire to understand the interaction of confined plasma with a container surface, an important element of research, which has the ultimate objective of achieving, controlled nuclear fusion. Surface collision studies have mainly involved the study of atomic or small (diatomic and triatomic) molecular ions impacting upon clean, well-characterized surfaces. In these studies, "low energy" ion-surface collisions have been defined by various authors as ranging from ~100 eV up to 10 keV. They address primarily physical mechanisms of the ion-

* Corresponding authors. E-mail: anil.shukla@pnl.gov; jean.futrell@pnl.gov

Our first article presenting a detailed study of the dynamics of surface induced dissociation, one of many subfields of mass spectrometry initiated by Graham Cooks, is dedicated to him on the occasion of his 60th birthday honoring his pioneering contributions to every aspect of mass spectrometry, especially to tandem mass spectrometry, the core of our research for many years.

PII S1387-3806(01)00509-7

surface interaction; namely, elastic scattering, ionization, neutralization, and excitation (inelastic scattering and sputtering). Recent investigations [8–12] have extended this inquiry to the "hyperthermal" energy regime below 100 eV. At these low collision energies, chemical interactions increase in relative importance, including surface trapping, dissociative adsorption, surface reaction, reactive scattering, and dissociative scattering.

Ion-surface collisions have been investigated with very different objectives by mass spectroscopists who employed hyperthermal collisions of large polyatomic ions with surfaces as an alternate ion activation method in tandem mass spectrometry [3,4]. Ion activation became an important process in the mass spectrometry field with the advent of the "soft" ionization/vaporization techniques, electrospray, and matrix assisted laser desorption ionization (MALDI). These techniques have extended mass spectrometry to large organic and biological molecules where the traditionally employed ionization/vaporization techniques (thermal desorption, etc.) decomposed these low vapor pressure, thermally fragile species. However, MALDI and electrospray have the corollary property that they generate mainly quasimolecular ions and only the mass of the precursor molecule is generally established in single stage mass analyzers. Tandem mass spectrometry generates invaluable connectivity information on "primary" ion mass selection with ion activation and subsequent mass analysis of the resulting "secondary" fragments. By separating fragmentation from ion production, tandem mass spectrometry is an invaluable technique for the analysis of high molecular weight organic and biological compounds, providing substantial insight into the arrangement of molecular groups that comprise high-mass bio-molecules.

The most commonly employed activation method in tandem mass spectrometry has been collision-induced dissociation (CID). In this technique a mass selected primary ion beam is passed through a cell where collision with a nonreactive target gas is used to convert small amounts of translational energy into internal (vibrational) energy of the primary ion. Because CID is momentum transfer limited, maximum of the laboratory frame collision energy that may be converted to ion internal energy is the center-of-mass (CM) energy of the two collision partners. With practical limits to the accelerating potential that may be applied to the primary ion beam, this becomes a severe limitation for high mass ions for which the mass ratio of the projectile ion to that of the neutral collider severely limits the energy available for transfer. Pragmatically it is difficult to obtain fragmentation sufficient to deduce useful structural information for ions heavier than 3500 daltons [13]. More efficient parent ion fragmentation may be realized in CID by employing multiple collisions to deposit larger total amounts of internal energy [14]. This is a particularly useful technique in Fourier transform ion cyclotron mass spectrometry (FTICR) where the number of collisions is, in principle, unlimited. However, high-energy fragmentation channels are inaccessible if there are competing low energy fragmentation channels that siphon off deposited internal energy before a sufficient amount for dissociation can accumulate. Finally radiative cooling is a competing process in any slow activation method, including CID.

The CM limitation in CID may be circumvented, in principle, by impacting an ion with a more massive collision partner. The limiting case is obviously collision with a rigid surface (infinite mass) for which energy conversion equal to the full laboratory frame energy is possible, in principle. Activation of polyatomic ions to induce their dissociation is referred to as surface-induced dissociation (SID)- equivalent to dissociative scattering in surface physics studies. In practice, bonds between surface atoms are not rigid and recent work reported by our laboratory has shown that SID may be described in terms of an effective surface mass [15]. Thus, the infinite mass limit of full conversion of ion translational energy into internal energy may never be realized in practice. Nevertheless, Cooks and coworkers have concluded that SID deposits a substantially greater amount and a narrower distribution of internal energy into the impacting ion, resulting in greater and more selective fragmentation than collision with a gas phase target in CID [16–19]. SID has been demonstrated to be an extremely effec-

tive means for dissociating large biological molecules [20]

Zhong and coworkers [21] have compared the fragmentation of the benzene molecular ion by single collision CID with SID on the same FTICR instrument and demonstrated that SID provides much higher energy deposition and a narrower internal energy distribution than CID. Consistent with other molecules studied in similar detail [22–24] energy deposition in high energy CID is much less than the CM collision energy limit and changes only slowly above 50 eV. At keV collision energy, for example, undissociated parent ions still remain the major constituent in the CID spectra [23,24]. In contrast with CID the SID, in FT-ICR results [14,21] rapid depletion of the parent ion (by 20 eV impact energy it is no longer the most intense ion signal) and extensive selective fragmentation (at 40 eV impact energy high-energy fragmentation channels dominate the mass spectrum). Hence, by judicious choice of accelerating potential the relative intensity of the various fragmentation channels may be selected. Laskin, Denison, and Futrell [15] have reported a more recent comparative study of the CID and SID of protonated dialanine on a FTICR instrument. By modeling their data using Rice–Ramsperger–Kassel–Marcus/quasiequilibrium theories they concluded that internal energy distributions of these ions by multiple collisional activation with a gaseous neutral and single collision with a self assembled monolayer (SAM) surface are very similar. Similarly broad internal energy distributions, were deduced by Rakov et al. [25], using a closely related method to deduce internal energy distributions from the energy dependence of ion fragmentation

As in the FTICR studies just mentioned [21,25], the present investigation of benzene cation dissociation utilizes a fluorocarbon SAM on a gold surface. It has been demonstrated that SAMs have significant advantages as SID surfaces [19,26–31]. Such SAM surfaces are easily prepared by immersion of a gold or silver substrate in a dilute solution of alkane thiol monomer in ethanol. The alkylthiol chains spontaneously assemble into highly ordered domains, covalently bonded to the metal surface through sulfur [32–34]. The resulting surface is stable in air, relatively well characterized, reproducible, and conveniently prepared. Somogyi and coworkers [27] found that increasing the chain length of the n-alkanethiol, $CH_3(CH_2)_nSH$, by n = 3,11, and 17 decreased both ion neutralization and surface reactivity. It was suggested that the special efficiency of perfluoro alkanethiols in SID reflects both their increased ionization energy (relative to hydrocarbon SAMs and oil films) and the increased mass of the end groups, whereas the stronger C–F bond suppresses surface reactivity.

Cooks and coworkers [16] have plausibly asserted that SID is quite similar to gas phase CID processes in that dissociation occurs after collisional activation; that is, the two processes are separated in time and dissociation occurs after the activated ion has recoiled from the surface. Burroghs and coworkers [35] have further elaborated this mechanism to describe it as a three-step process, viz., impulsive excitation, inelastic reflection, and unimolecular dissociation of the activated ion. The second step of inelastic reflection is associated with energy loss to the surface. An alternative SID mechanism in which the ion dissociates on impact with the surface, i.e., very fast dissociation on or in the proximity of the surface, is termed “shattering.” Relative to the present research, the two (or three) step and shattering mechanisms are easily distinguished experimentally by measuring kinetic energies (hence velocity) of the fragment ions. In the two/three step SID process, all fragment ions have the same velocity (resulting from unimolecular decay of the excited parent ion) whereas fast dissociation on the surface gives rise to fragments with different velocity, often with the same kinetic energy of recoil from the surface. Both types of SID processes are predicted theoretically and have been reported in the literature.

Recent investigations by Herman and coworkers [36,37] of the dynamics of impact of benzene and ethanol molecular ions with polished stainless steel surfaces (coated with an adlayer of pump oil) have reported full resolution of angular and kinetic energy distributions for both reactive and inelastic scattering in SID. In this complementary study we present the angle and energy resolved impact of benzene molec-

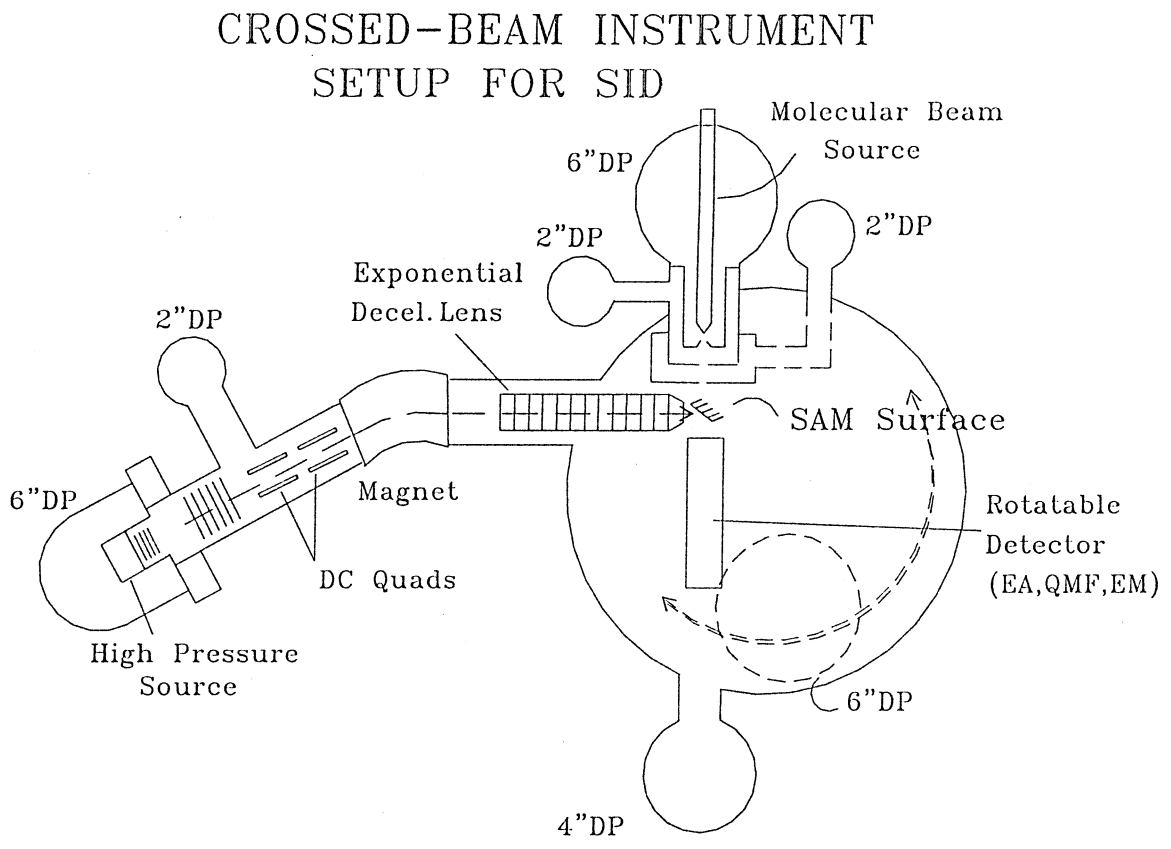

Fig. 1. Schematics of the crossed-beam instrument modified and used for the surface-induced dissociation studies described in this paper.

ular ion with a fluorinated alkanethiolate SAM surface, 2-(perfluorodecyl) ethanethiol ($CF_3(CF_2)_9CH_2CH_2SH$). This work broadens our understanding of the dynamics of SID and complements our group's previous and ongoing Fourier transform mass spectrometry-SAM-SID investigations of benzene and model peptides.

2. Experimental

Surface impact was carried out in a modified crossed-beam scattering instrument shown schematically in Fig. 1. This apparatus has been used previously to study ion-molecule reaction dynamics of various processes in gas phase collisions and has been described in detail [38]. Briefly, the system consists of a means for producing a mass-analyzed, low energy ion beam that intersects a supersonic molecular beam. A detector assembly, which may be rotated about an axis located at the intersection of the crossed beams, performs product mass and energy analysis. This apparatus was modified for SID studies by placing a perpendicular surface mounted at the ion beam-neutral beam crossing point. Thus, all SID measurements were conducted using an in-plane scattering geometry in which the three axes' defined by the primary ion beam, surface normal, and product ion detection are coplanar. The surface mount was designed so that surface may be oriented at 15°, 30°, or 45° with respect to the ion beam axis, if desired. The present study was conducted with only an impact angle of 45°.

Primary ions were created in a high-pressure (~1 Torr of benzene vapor) high-energy electron impact

(750 eV) source maintained at a voltage close to the desired ion energy. The ions formed inside the source block undergo a large number of collisions with neutrals and secondary electrons, resulting in their relaxation to the ground state with minimal internal excitation. The ion-neutral collisions also result in the formation of a significant number of benzene dimer ions. Ions were extracted, accelerated to a 750 eV translational energy and passed through a magnetic sector, operated as a mass filter, where selection of the ion of interest occurs. The mass-selected primary ion beam was then decelerated to desired collision energies by an exponential deceleration lens and focused onto the surface maintained at ground potential.

Scattered primary ions and fragment ions were energy analyzed, mass selected, and detected by a 90° cylindrical electrostatic energy analyzer, quadrupole mass filter, and an electron multiplier operated in pulse counting mode, respectively. This assembly can be rotated with respect to the collision center to measure kinetic energy distributions for angles ranging from 0° to 95° with respect to the incoming ion beam. In the present experiments the orientation of the surface "shadows" the first 45° of the detector travel. Hence, kinetic energy distributions of product ions were measured from the surface plane at 45° to the end of the assembly travel at 95° (for 45° ion-surface impact 90° is the elastic scattering specular angle). Accordingly, with this apparatus we record translational energy spectra (product ion kinetic energy distributions) parameterized by primary ion impact energy, primary ion impact angle, product ion mass, and product ion scattering angle. Using these spectra to plot product ion intensity vs. collection angle an angular mass intensity plot is produced. By integrating over all angles for each product ion a "conventional" SID mass spectrum may be generated.

The 2-(perfluorodecyl)ethanethiol ($CF_3(CF_2)_9CH_2CH_2SH$) SAM surface was prepared by immersing a gold coated metal surface in a 1mM solution of fluorinated alkanethiol in ethanol for ~24 h, to allow sufficient time for well ordered self assembly of the monomer alkyl chains to be formed. The fluorinated alkanethiol, $CF_3(CF_2)_9CH_2CH_2SH$, was obtained from the laboratory of Professor Wysocki at the University of Arizona where it was synthesized and tested for purity using standard methods. The gold-coated surfaces were obtained from Evaporated Metal Films (Ithaca, NY) which were fabricated by vapor deposition of gold to a thickness of about 1000 Å on a titanium-coated silica substrate. The gold surface was cleaned twice by exposure to UV light and in an ultrasonic cleaner in absolute ethanol for 15 min each prior to immersion. Spectroscopic grade benzene was obtained from the Aldrich chemical company and used without further purification.

Oil diffusion pumps equipped with water-cooled baffles pumped all the ion source, flight tube, and collision chamber. The background pressure in the collision chamber was $\sim 8\times10^{-8}$ Torr after overnight pumping of the chamber and did not increase with the introduction of gas in the source.

The kinetic energy and angular distributions of the primary ion beam at different kinetic energies were measured before the start of SID experiments by bringing the detector assembly in-line with the ion beam direction. The ion beam tuning conditions were maintained as close to these conditions for the rest of experiments. Typically, the ion beam had energy spread of ~1.5 eV [full width at half maximum (FWHM)] and angular spread of ~2° (FWHM) for 50 eV energy ions.

All experiments were repeated several times over a period of many months. Because of our concern about damage to the surface by continuous ion impact, we replaced the surface regularly (once a week or more, if the system was vented for any reason) and repeated experiments at a few angles previously examined to confirm reproducibility of our experimental data. The tuning of the ion beam was maintained as constant as possible between experiments with particular emphasis to reduce beam steering voltages to low values. The ion energy range for SID experiments was limited to 10 eV and higher since the fragment ion intensities below this energy were too weak to obtain statistically reliable data within a reasonable period of time. For the same reason we restricted the present study to the two most abundant fragment ions, *m/z* 52 and *m/z* 39, even though *m/z* 77 fragment is the lowest energy dissociation product. The high intensity of the pri-

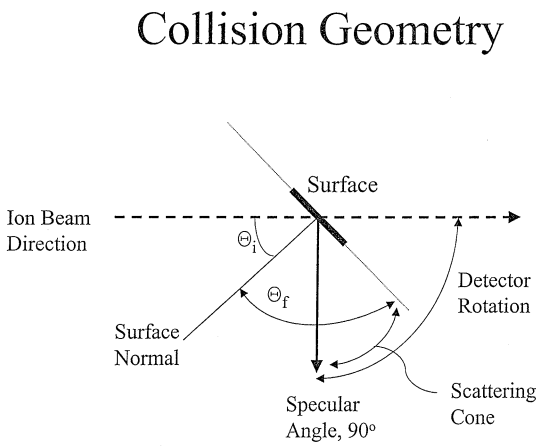

Fig. 2. Collision geometry and definition of incident angle and scattering angle used in the present study.

mary ion peak at *m/z* 78 made it extremely difficult to obtain unbiased energy distributions for *m/z* 77 with quadrupoles as the mass filter.

Our experimental data are presented following the surface science convention in which the angle of incidence, θ_i, and angle of detection (scattering), θ_f, are measured with respect to the surface normal as schematically shown in Fig. 2.

3. Results and discussion

We begin this section with the results from our lowest translational energy experiments at which SID fragment ions are detected, 10 eV. At this energy no elastically scattered primary ions are detected- only highly inelastically scattered parent ions and fragment ions are found. Fig. 3 shows the translational energy distributions of inelastically scattered benzene ions and the two most abundant fragment ions at mass 52 and 39. These distributions were recorded at 65° scattering angle. Several unusual features are clearly obvious from this figure. First, the inelastically scattered parent ion peak is broader than the fragment ion peaks even though these latter peaks are broadened by kinetic energy release on dissociation. Secondly, the inelastically scattered primary ion peak is shifted to a lower kinetic energy than the two fragment ion peaks

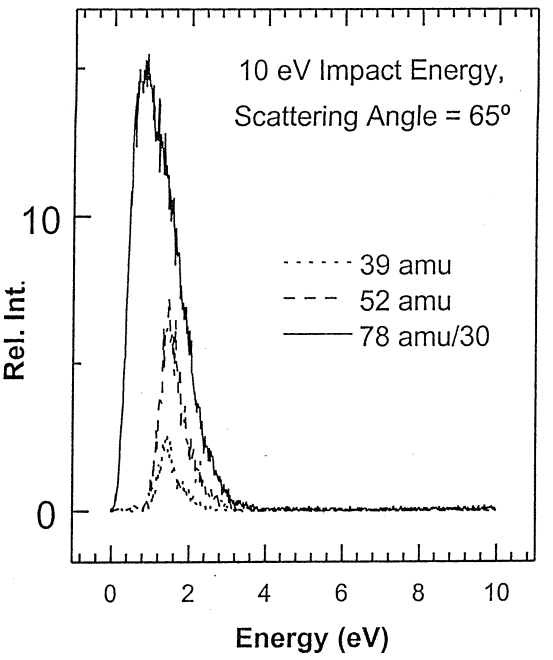

Fig. 3. Translational energy distributions of undissociated benzene ions and fragment ions, *m/z* 52 and *m/z* 39, from collisions of 10 eV energy primary benzene ions and collected at a fixed scattering angle of 65°.

in spite of the fact that the two fragmentation processes are highly inelastic (endothermic by 4.4 and 4.5 eV, respectively). Assuming that primary ions are not internally excited and that excited ions decompose at threshold, inelastically scattered ions at the peak maximum have a 0.8 eV translational energy and a maximum of 3.7 eV internal energy (corresponding to the lowest energy dissociation threshold, loss of H to form $C_6H_5^+$). This corresponds to a minimum energy transfer of 5.5 eV kinetic energy lost by the colliding ions into the surface excitation. If the scattered benzene ions have lower internal energies, more than 5.5 eV goes into the surface modes. From this analysis of scattered ion kinetic energies it is apparent that the SAM surface is a very efficient sink for translational energy.

We can analyze the kinetic energy spectra of the two fragment ions at 10 eV collision energy in the same manner. From the peak positions, we estimate the most probable energy losses of 7.0 and 7.6 eV for

benzene ions recoiling from the surface and decomposing into $C_3H_3^+$ and $C_4H_4^+$ fragment ions, respectively. Since the thermochemical thresholds for the two processes are 4.4 and 4.5 eV, respectively, we conclude that the most probable energy transferred into the surface corresponds to 2.6 and 3.1 eV for $C_3H_3^+$ and $C_4H_4^+$ fragment ions, respectively.

It is interesting to note that the kinetic energy distributions of fragment ions do not match that of inelastically scattered benzene cations. Rather they match approximately the higher energy "shoulder" of the benzene cation scattered intensity. It will be demonstrated in subsequent discussion that three mechanisms are involved in the nondissociative scattering of benzene cations by SAM surfaces. They result, respectively, in peaks corresponding to thermalization (stick collisions, possibly involving multiple encounters, principal inelastic scattering mechanism, and elastic scattering). The simplest interpretation of Fig. 3 is that two overlapping mechanisms contribute to the observed inelastic scattering at 10 eV- namely, thermalization and the principal inelastic scattering mechanisms. According to this interpretation, the high-energy shoulder kinetic energy distribution is mirrored by that of the detected fragment ions in the principal inelastic scattering mechanism. It will be shown for higher energy experiments that this mechanism results in parent and fragment ions having the same velocity. Intensity of fragment ions is too low at 10 eV for us to demonstrate this mechanism conclusively.

Fig. 4 shows the angular distributions of fragment ions and undissociated primary ions as a function of primary ion kinetic energy. The amount of fragmentation of the impacting ion is very small, at 10 eV collision energy, but increases with collision energy. Because of the low signal of fragment ions at 10 eV, measurements of fragment ion translational energy spectra could be made at only a few angles. At 20 eV impact energy (not shown) fragmentation has increased to approximately 10% of the intensity of undissociated, inelastically scattered primary ions. At 50 eV ion energy fragmentation is of the order of 50% of undissociated primary ions. Thus, the relative abundance of the two fragment ions increases with the ion kinetic energy.

For all impact energies the angular distribution of both undissociated primary ion and fragment ions lies substantially closer to the surface than the $\theta_f = 45°$ specular angle. The lobe positions shift from close to the surface towards the specular angle with increasing impact energy. In the 10 eV angular distribution the lobe maximum of undissociated primary ions is located at $\theta_f \sim 70°$. At 20 eV both scattered primary ions and fragment ions leave the surface at $\theta_f \sim 60°$, 30° above the surface plane. At 50 eV the angular distributions are very broad and there is evidence at this energy for a bimodal distributions. The intensity maxima are also shifted from each other but do not approach the specular angle at any impact energy investigated.

Translational energy spectra of undissociated benzene cations and $C_3H_3^+$ and $C_4H_4^+$ fragment ions were recorded every 5° from the surface plane at $\theta_f = 95°$ to the specular angle at $\theta_f = 45°$. Fig. 5 compares the translational energy spectra of undissociated benzene radical cations recorded at $\theta_f = 70°$ for each of the three impact energies investigated. The translational energy spectra of undissociated benzene ions for three impact energies are quite different. At 10 eV collision energy, scattered benzene cations leave the surface with a most probable translational energy of 1 eV (energy loss of ~90%) whereas 20 and 50 eV benzene cations leave with most probable kinetic energies of 6 eV (loss of 70%) and 18 eV (loss of 64%), respectively. An interesting feature in these spectra is that the 20 and 50 eV spectra have multiple peaks; two peaks are observed at 20 eV and three peaks of quite different relative abundances at 50 eV. At 20 eV, the most probable low energy is 6 eV but a clearly discernible shoulder corresponds to about 1 eV kinetic energy. At 50 eV the <1 eV peak and an elastic recoil peak at ~50 eV are well separated from the main peak at about 18 eV.

The angular dependence of these three peaks was investigated at 50 eV, for which all three energies are clearly resolved. The results are summarized in Fig. 6. At 60° (near the maximum intensity) the relative intensities of the low energy (highly inelastic, <1 eV

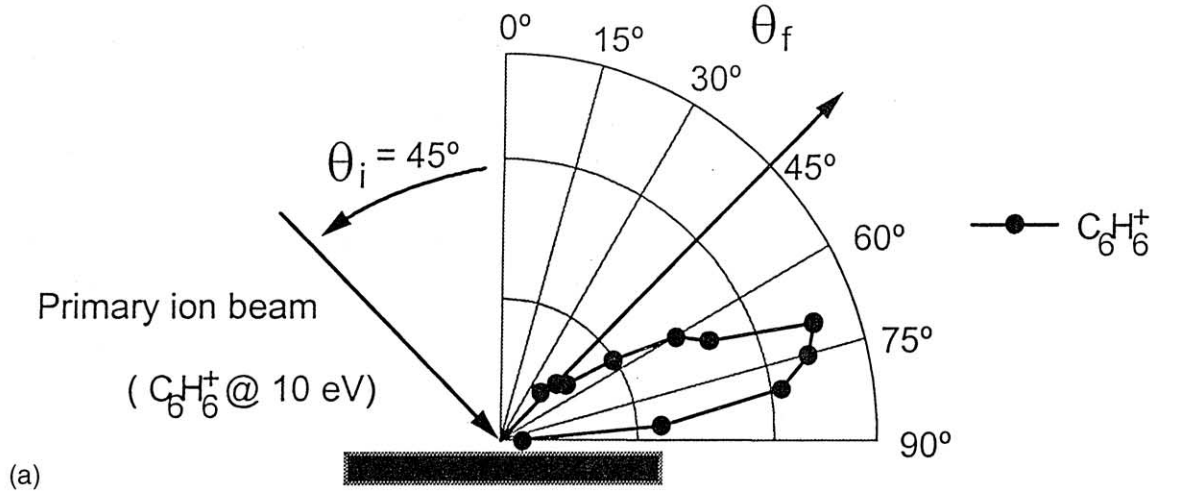

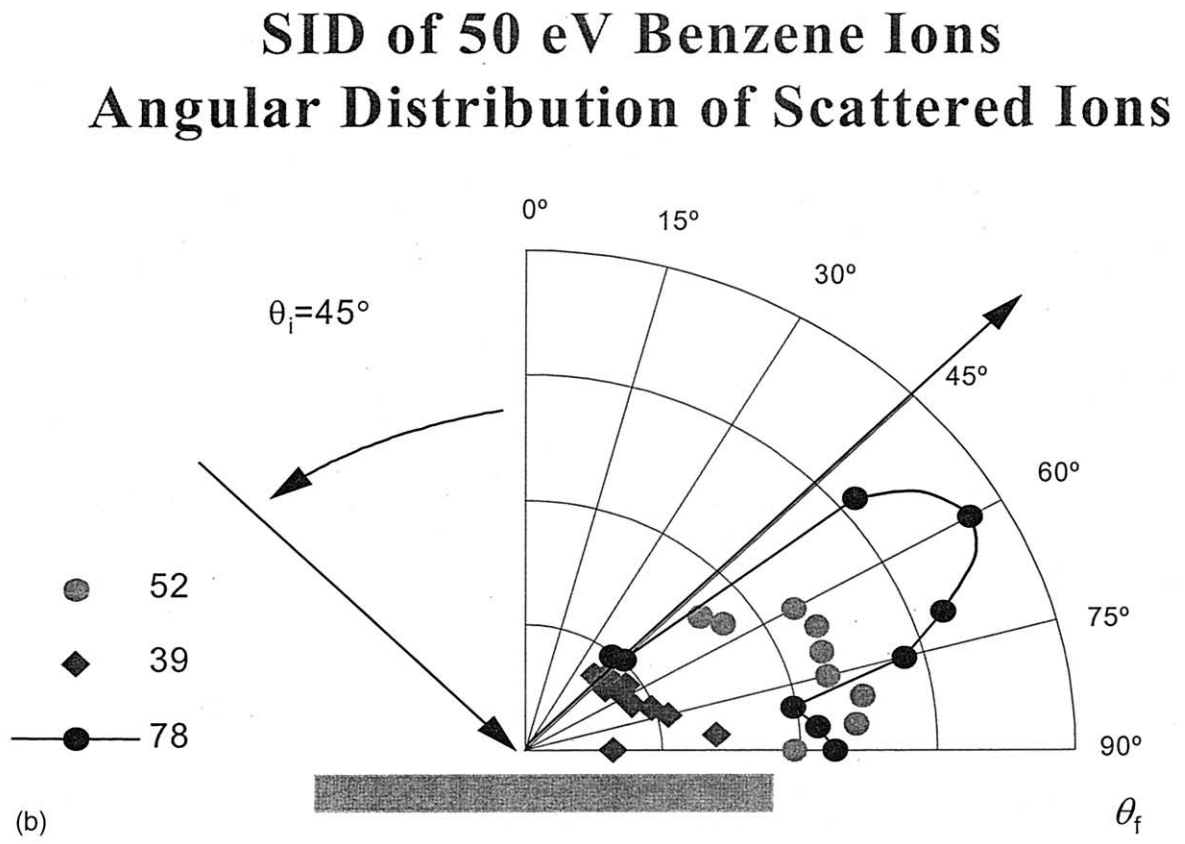

Fig. 4. Angular distributions of undissociated benzene ions and fragment ions, *m/z* 52 and *m/z* 39, as a function of the ion's kinetic energy at (a) 10 and (b) 50 eV collision energies.

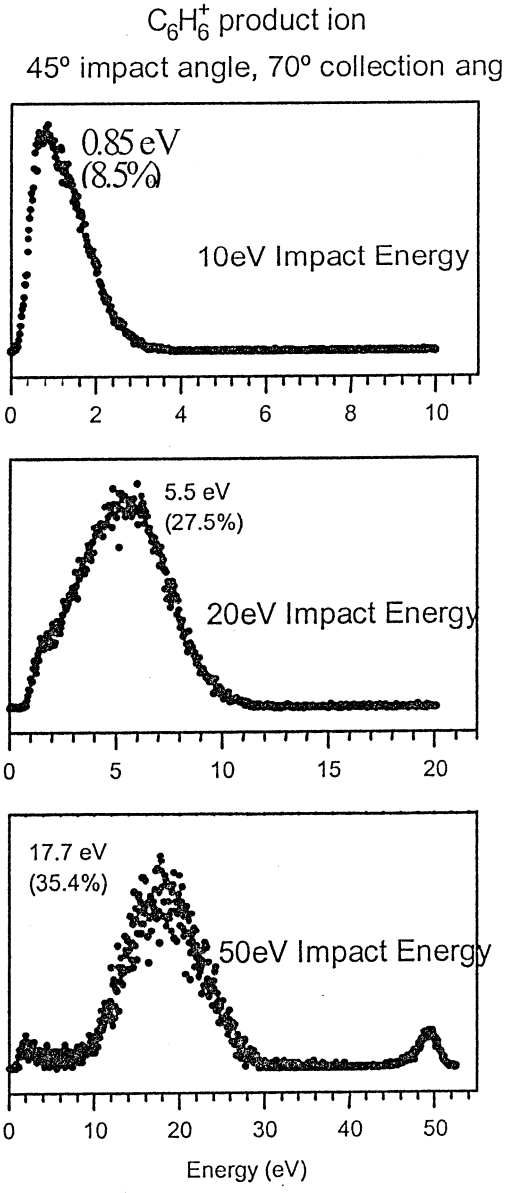

Fig. 5. Translational energy distributions of undissociated benzene ions scattered off the surface at 70° fixed scattering angle and primary ion energies of 10, 20, and 50 eV primary ion beam energies.

recoil energy) and elastic (~50 eV, no measurable energy loss detected) peak and the main peak are similar to that already shown for 70° scattering. At larger recoil angles 75° and 85°, the latter being

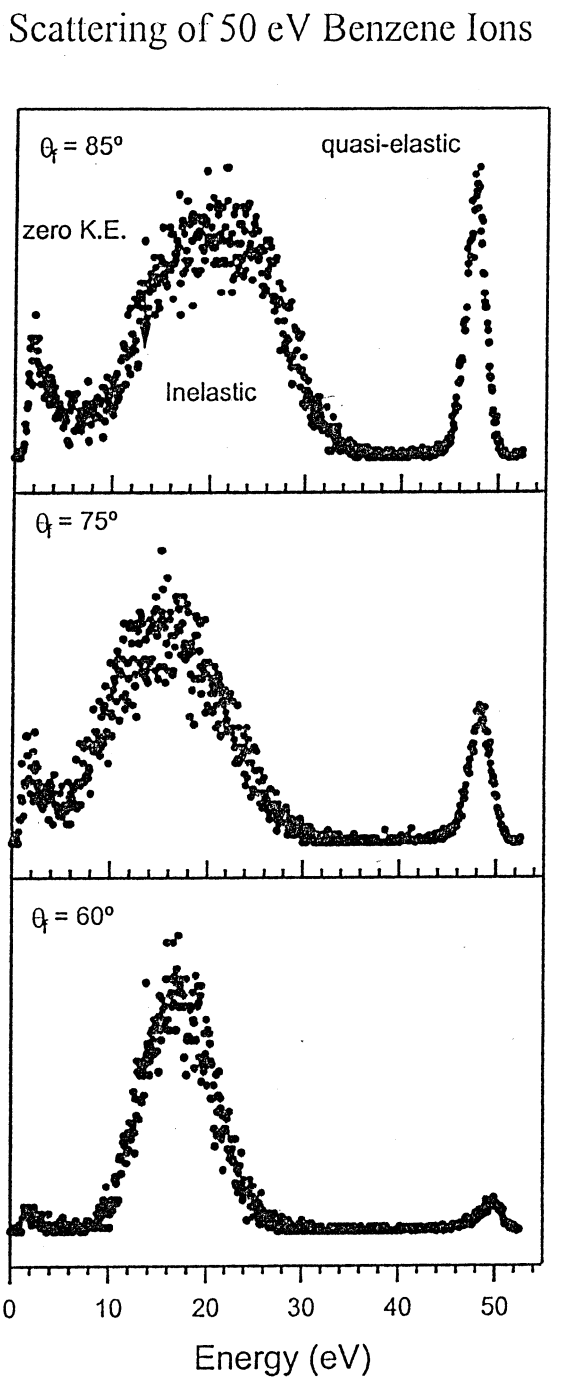

Fig. 6. Translational energy spectra of undissociated benzene ions at 60, 75, and 85° scattering angles from collision of 50 eV kinetic energy primary benzene ions.

nearly parallel to the surface, the relative intensities of both the high energy (quasielastic) and low energy (quasithermalized) peaks increase dramatically.

The higher energy peaks have clear analogies to gas phase collisions and will be discussed below. The quasithermal peak is specific to scattering by the SAM surface. It represents multiple collisions with a soft surface in which essentially all translational energy is lost to surface modes and the ion recoils with very low translational energy. This mechanism can be identified with ion capture on the surface at lower impact energy, as described by Miller and coworkers [39]. These workers demonstrated that organic ions could be captured ("stuck" or "soft landed") on (or in) the SAM surface, that such stored ions were stable for long periods of time and that they could be released by sputtering with high-energy argon ions. The present mechanism likely represents thermalization of the impacting ion with localized heating of the impact area that causes a moderate fraction of the ions to leave the surface. Thus, it corresponds to the combination of the ion storage and release mechanisms investigated by Miller and coworkers [39].

The relatively sharp quasielastic peak, which is strongly forward scattered, corresponds to elastic scattering in gas phase collisions. It results from a single (or a few, if a "skipping" mechanism applies) relatively larger impact parameter glancing collisions. The maximum intensity is parallel to the surface and decreases relatively steeply as the detector is rotated away from the surface plane. In the gas phase elastic scattering is strongly forward peaked, as is this SID mechanism. Complete forward scattering is masked by the surface and the observed peak of intensity parallel to the surface is analogous to the wings of the forward scattered elastic peak in gas phase collisions.

The scattering cones for inelastically scattered parent ions and fragment ions (Fig. 4) are relatively narrow and similar to typical gas phase CID scattering results [40]. This strongly suggests the main features of SID involve scattering by surface groups of atoms rather than, for example, entire alkyl chains or strongly coupled ensembles of atoms in the two-dimensional (2D) crystal SAM structure. It is therefore instructive to apply two-body scattering theory to the most probable momentum exchange mechanisms. Applying standard conservation of energy and angular momentum the energy of the projectile ion after a single collision is [41]

$$E_f/E_i = [\cos\theta + (\mu^2 - \sin^2\theta)^{1/2}]^2/(1+\mu)^2 \quad (1)$$

where $\mu = m_T/m_p$, ratio of the mass of the target and the projectile, E_f and E_i are the final and initial energies, respectively, of the projectile ion and θ is the angle of the projectile ion's deflection from the initial beam direction. Substituting experimental data for initial and final energies at $\theta = 60°$ and solving for μ one obtains $\mu = 1.5$, from which the mass of the target particle is calculated to be 117. This is very close to the mass of the terminal CF_2CF_3 group, 119 amu, of the fluorinated alkyl SAM surface. Similarly, we obtain $\mu = 1.44$ for the dissociative scattering of benzene cation to *m/z* 52 fragment ions, corresponding to a target mass of 112 which is not too far off from the mass of the C_2F_5 chain at the end of the SAM surface. We therefore infer that the principal scatterer in these experiments is the perfluoroethyl group.

Analogous measurements by Koppers et al. [42,43] of angular and energy distributions of positive and negative ions from dissociative scattering of CF_3^+ off a liquid insulating perfluorinated polyether surface on stainless steel substrate and scattering/dissociative scattering of C^+, CF^+, CF_2^+, and CF_3^+ from the same surface have reached similar conclusions about scattering dynamics. In the perfluorinated polyether the annealed surface is "knobby," with CF_3 groups exposed to the vacuum interface. Their dissociative scattering data were interpreted as involving these exposed CF_3 groups as the momentum conserving scattering moiety. As discussed in detail by these workers, this kind of scattering is remarkably different for a fluorocarbon soft surface from ion/metal surface scattering. It is noteworthy that in our recent SID studies [44] of CS_2^+ ions on the same fluorinated alkanethiol SAM surface as used in our benzene SID reported here, the binary collision model, described by Eq. (1), suggests that the CF_3 end group in the

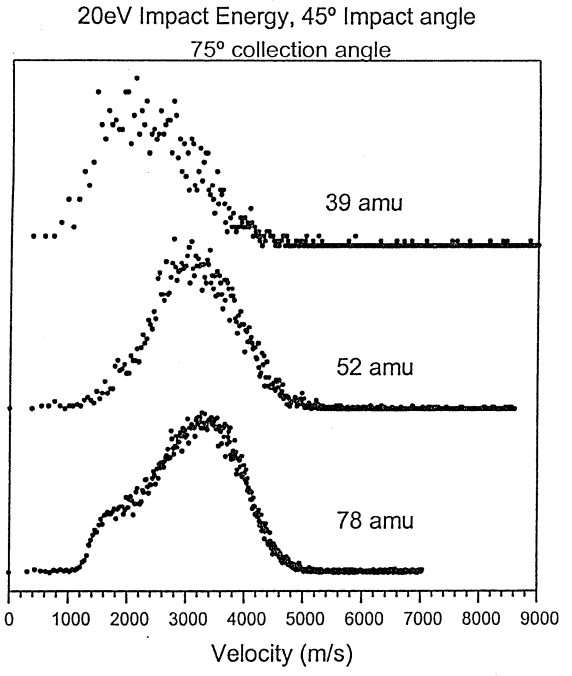

Fig. 7. Velocity distributions of undissociated benzene ions and fragment ions, *m/z* 52 and *m/z* 39, from collision of 20 eV energy benzene ions and measured at 75° scattering angle.

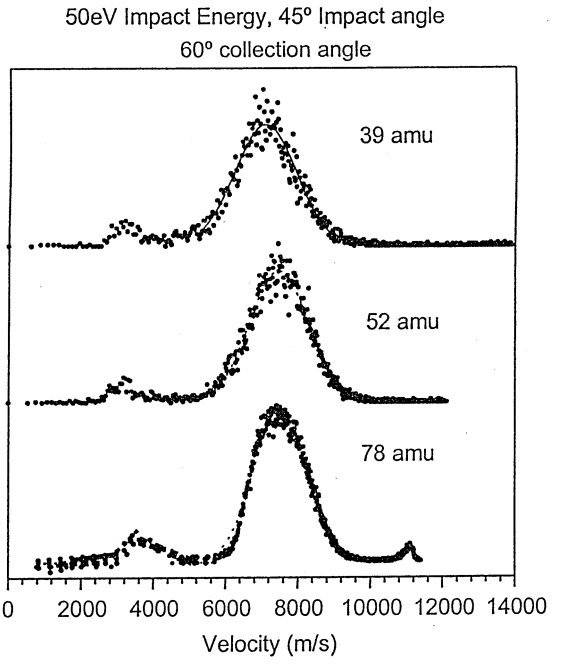

Fig. 8. Velocity distributions of undissociated benzene ions and fragment ions, *m/z* 52 and *m/z* 39, measured at 60° scattering angle. These velocity distributions were obtained by converting measured kinetic energy distributions into velocity distributions using the relationship $E = \frac{1}{2}\,mv^2$.

fluorinated alkyl chain is the effective moiety for scattering and SID.

We now discuss the fragmentation processes at 20 and 50 eV impact energies. We begin by converting the translational energy distribution curves to velocity distributions using the relationship $E = \frac{1}{2}\,mv^2$. Fig. 7 shows the velocity translational energy distributions of the fragment ions at 20 eV impact energy and 75° scattering angle along with the velocity distribution for undissociated primary ions. It is immediately apparent that velocity distributions of the undissociated benzene ions and $C_4H_4^+$ fragment ions are very similar whereas that of $C_3H_3^+$ fragment ions is very broad and overlaps the velocity distributions associated with the main peak and the low velocity peak in the spectrum of the undissociated primary ions. Asymmetric and broadened velocity distribution for $C_3H_3^+$ suggests that both groups of inelastically scattered benzene ions exhibit this dissociation channel.

As already noted the 50 eV data for inelastically scattered $C_6H_6^+$ clearly separate into three mechanistic groups. Fig. 8 presents the 50 eV incident energy kinetic energy spectra converted to velocity distributions for $C_3H_3^+$ and $C_4H_4^+$ fragment ions and compares their velocities to scattered $C_6H_6^+$ primary ions. All three ions leave the surface at close to 7 500 m/s. The lower intensity peaks corresponding to nearly full energy transfer are also observed to have essentially the same velocities. From Figs. 7 and 8 we can conclude that most, if not all, dissociation of benzene ions takes place after the collisionally excited ions recoil from the surface. If the ions dissociated on surface impact, i.e. “shattered” on collision with the surface, we would see no correlation with undissociated but internally excited molecular benzene cations. From the maximum of these distributions, we determine that SID for *m/z* 52 corresponds to energy loss of 16 ± 1 eV whereas that for *m/z* 39 fragment ion corresponds to loss of 18 ± 1 eV. We have already

deduced that only a small fraction of this energy is transferred into internal modes leading to dissociation.

It is also of interest in Fig. 8 that the velocity distributions of fragment ions track both inelastic mechanisms, both the main peak and the quasithermal peak. This expected result confirms the two-step mechanism for SID. As also expected, no fragment ions match the quasielastic peak. This confirms that the high-pressure source has quenched any excited states formed in the ionization process and that elastic scattering is not accompanied by unimolecular decay of the scattered benzene cations [45].

It is noteworthy that fragment ions at *m/z* 51 and *m/z* 50 were not detected in significant abundances. This is at first surprising since they are quite abundant in all other SID studies at 50 eV ion energy. One possible rationale for this discrepancy may be very tight energy, mass, and angular resolutions in our experiments. In particular, the collection efficiency of ions scattered at larger angles in a three-dimensional (3D) scattering plane is drastically reduced since the 2D detector samples only a small fraction of the 3D scattering cone. Previous results which detected substantial *m/z* 50 and 51 products involved quadrupoles or ion traps, both of which have very large acceptance angle and in all likelihood collect majority of scattered ions in a 3D plane (and lose scattering information in the process). We cannot rule out the possibility of scattering losses and/or instrumental discrimination to account for the near absence of these lower energy processes in our dynamics studies.

We further note that the angular scattering characteristics shown in Fig. 4 are complementary in all respects with the results reported by Wörgötter and coworkers for the dynamics of SID of benzene and ethanol cations measured for an oil-film coated stainless steel surface [36,37]. Moreover, these same general features are found for SID of ethanol cations on collision with the same SAM surface [45] investigated in the present research. Of particular interest is the fact that a simple dynamics model accounts for the angular scattering characteristics of parent and product ions. As the angle of incidence was varied from 80° to 60° to 40°, inelastically scattered parent and fragment ions maximized previously, at and below the specular scattering angle [37]. This was explained by their observation that ion velocity parallel to the surface was constant and the perpendicular component changed with both impact energy and angle. The perpendicular component was small (e.g. highly inelastic) and proportional to primary ion kinetic energy. Although our study was limited to a single angle of incidence (and a different cation) our results are consistent with Wörgötter's model. Specifically the smaller component of perpendicular velocity at 45° pulls the scattering angle for inelastically scattered benzene ions and their fragment ions below the specular scattering angle.

Assuming this model also helps in reconciling our previously published work in which benzene cations were impacted on a SAM surface inside an ICR cell at normal incidence. Specifically our earlier report of the very efficient conversion of translational energy into internal energy appears to contradict the more modest increase of fragmentation with impact energy reported here. However, relating the earlier normal incidence study to the normal component of energy in the present experiments reconciles our two classes of experiments, both of which used relaxed benzene ions as projectiles.

In focusing attention on SID one should not forget that neutralization of primary ions is by far the dominant reaction channel in ion-surface collisions, even when F-SAM surfaces are utilized as the collider. Earlier studies of benzene ion SID have reported fragmentation efficiency varying between 10% and 30%. Neither our experimental measurements nor the beam studies of Kubišta and coworkers [37] support such high SID efficiency. Our experiments continuously monitored the ion beam current on the surface using an electrometer, which can readily be compared with the total count rate of energy, mass, and angle-resolved ions. The overall transmission efficiency of our detector is of the order of 10^{-3}, which precludes an accurate estimate of SID efficiency. However, our best estimate of the integrated secondary signal for 50 eV collisions is of the order of less than one percent rather than tens of percents. This is much less than we reported for normal incidence SID inside an ICR cell

[21]. In both the present experiments and in Wörgötter's beam studies, ions must travel a few centimeters under field-free conditions with no magnetic or electric fields to ensure capture of all or most secondary ions. The hypothesis of large angle scattering at or near the surface is the only suggestion we can presently offer as an explanation. Further research is required and we hope that experiments carried out in our laboratory in the near future will resolve this issue.

4. Conclusions

Principal conclusions from the present study of the dissociative and inelastic scattering of benzene molecular ions can be summarized as follows. Charge neutralization is the dominant reaction channel at these energies even when the surface is modified by attaching a fluorinated alkyl SAM layer. Both SID and inelastic scattering processes result in nonspecular scattering at all energies studied. Energy lost by the projectile ions is very large and most energy is dissipated into surface modes. Due to the relatively strong coupling with a soft surface the dynamics are best described as resulting from pseudo-gas phase scattering by a surface moiety. A simple model suggests a C_2F_5 group as the momentum exchanging collider. After collisional activation the excited ion decomposes unimolecularly into fragments that have the same velocity as the recoiling, inelastically scattered parent ion. We observe three energetically distinct scattering modes for 50 eV energy collisions that are described as quasielastic, inelastic, and almost fully inelastic. SID processes correspond energetically with only the latter two inelastic processes and the contribution from the fully inelastic process to total SID is very small. This is direct evidence that the binary collision model can be extended to explain low energy ion-surface collisions of polyatomic ions.

It should be noted that internal excitation in the benzene cation when generated by electron impact frequently confounds the interpretation of energy transfer in collisional activation studies, including SID.

Acknowledgements

This research was supported by the National Science Foundation, Grant No. CHE- 9616711. The NSF- GOALI program (Grant No. CHE- 9634238) provided partial support for Dr. deClercq's tenure at the University of Delaware. We thank Professor Vicki Wysocki for providing us with the surface material synthesized in her laboratory and Professors Cooks, Wysocki, and Herman for many helpful discussions of SID phenomena. We also thank Dr. Zhong for her help in surface preparation and Drs. Laskin, Rakov, and Denisov for fruitful discussions, providing preprints of related articles and critical comments on the paper.

References

[1] N.H. Tolk, J.C. Tully, W. Heiland, C.W. White (Eds.), Inelastic Ion-Surface Collisions, Academic, New York, 1977.
[2] W. Eckstein, H. Verbeck, S. Datz, Appl. Phys. 27 (1975) 527.
[3] W. Heiland, W. Beitat, E. Taglauer, Phys. Rev. 19 (1979) 1677.
[4] B. Willerding, W. Heiland, K. J. Snowdon, Phys. Rev. Lett. 53 (1984) 2031.
[5] J.M. Zoest, C.E. van der Meij, J.M. Fluit, Nucl. Instrum. Methods Phys. Res. B 2 (1984) 406.
[6] M. Mannami, K. Kimura, K. Nakamishi, A. Nishimura, Nucl. Instrum. Methods Phys. Res. B 13 (1986) 587.
[7] W. Heiland, E. Taglauer, Nucl. Instrum. Methods 194 (1982) 667.
[8] J.W. Rabalais (Ed.), Low Energy Ion-Surface Interactions, Wiley, New York, 1994.
[9] Y. Murata, in Unimolecular and Bimolecular Reaction Dynamics, C.Y. Ng, T. Baer, I. Powis (Eds.), Wiley, New York, 1994, p. 428.
[10] H. Akazawa, Y. Murata, Phys. Rev. Lett. 61 (1988) 1218.
[11] H. Akazawa, Y. Murata, Phys. Rev. B 39 (1989) 3449.
[12] S.R. Kasi, H. Kang, C.S. Sass, J.W. Rabalais, Surf. Sci. Rep.10 (1989) 1.
[13] A.L. McCormack, A. Somogyi, A.R. Dongre, V.H. Wysocki, Anal. Chem. 65 (1993) 2859.
[14] J. Laskin, M. Byrd, J.H. Futrell, Int. J. Mass Spectrom. 195/196 (2000) 285.
[15] J. Laskin, E. Denisov, J. Futrell, J. Am. Chem. Soc. 122 (2000) 9703.
[16] R.G. Cooks, T. Ast, M.A. Mabud, Int. J. Mass Spectrom. Ion Processes 100 (1990) 209.
[17] S.A. Miller, D.E. Riederer Jr., R.G. Cooks, W.R. Cho, H.W. Lee, H. Kang, J. Phys. Chem. 98 (1994) 245.

[18] M.J. DeKrey, H.I. Kenttämaa, V.H. Wysocki, R.G. Cooks, Org. Mass Spectrom. 21 (1986) 193.
[19] R.G. Cooks, T. Ast, T. Pradeep, V.H. Wysocki, Acc. Chem. Res. 27 (1994) 321.
[20] A.R. Dongre, A. Somogyi, V.H. Wysocki, J. Mass Spectrom. 31 (1996) 339.
[21] W. Zhong, E.N. Nikolaev, J.H. Futrell, V.H. Wysocki, Anal. Chem. 69 (1997) 2496.
[22] A.K. Shukla, S.G. Anderson, K. Qian, J.H. Futrell, Int. J. Mass Spectrom. Ion Processes 109 (1991) 227.
[23] S.G. Anderson, Ph.D. Thesis, University of Utah, 1992.
[24] R. Chawla, A. Shukla, J. Futrell, Int. J. Mass Spectrom. Ion Processes 165/166 (1997) 237.
[25] V.S. Rakov, E.V. Denisov, J. Laskin, J.H. Futrell, J. Phys. Chem. submitted.
[26] V.H. Wysocki, J.-M. Ding, J.L. Jones, J.H. Callahan, F.L. King, J. Am. Soc. Mass Spectrom. 3 (1992) 27.
[27] A. Somogyi, T.E. Kane, J.-M. Ding, V.H. Wysocki, J. Am. Chem. Soc. 115 (1993) 5275.
[28] M. Morris, D.E. Riederer Jr., B.E. Winger, R.G. Cooks, T. Ast, C.E.D. Chidsey, Int. J. Mass Spectrom. Ion Processes 122 (1992) 181.
[29] B.E. Winger, R.K. Julian Jr., R.G. Cooks, C.E.D. Chidsey, J. Am. Chem. Soc. 113 (1991) 8967.
[30] V.H. Wysocki, J.L. Jones, J.-M. Ding, J. Am. Chem. Soc. 113 (1991) 8969.
[31] T.E. Kane, A. Somogyi, V.H. Wysocki, Org. Mass Spectrom. 28 (1993) 283.
[32] M.D. Porter, T.B. Bright, D.L. Allara, C.E.D. Chidsey, J. Am. Chem. Soc. 109 (1987) 3559.
[33] L. Strong, G.M. Whitesides, Langmuir 4 (1988) 546.
[34] H.O. Finklea, D.D. Hanshew, J. Am. Chem. Soc. 114 (1992) 3173.
[35] J.A. Burroghs, S.B. Wainhaus, L. Hanley, J. Phys. Chem. 98 (1994) 10913.
[36] R. Wörgötter, J. Kubišta, J. fabka, Z. Dolejšek, T.D. Märk, Z. Herman, Int. J. Mass Spectrom. Ion Processes 174 (1998) 53.
[37] J. Kubišta, Z. Dolejšek, Z. Herman, Eur. Mass Spectrom. 4 (1998) 311.
[38] M.L. Vestal, C.R. Blakley, P.W. Ryan, J.H. Futrell, Rev. Sci Instrum. 47 (1976) 15.
[39] S.A. Miller, H. Luo, S. Pachuta, R.G. Cooks, Science 275 (1997) 1447.
[40] A.K. Shukla, J.H. Futrell, J. Mass Spectrom. 35 (2000) 1069.
[41] U. Gerlach-Meyer, E. Hulpke, in Topics in Surface Chemistry, E. Kay, P.S. Bagus (Eds.), Plenum, New York, 1978.
[42] W.R. Koppers, J.H.M. Beijersbergen, T.L. Weeding, P.G. Kistemaker, A.W. Kleyn, J. Chem. Phys. 107 (1997) 10736.
[43] W.R. Koppers, M.A. Gleeson, J. Lourenco, T.L. Weeding, J. Los, A.W. Kleyn, J. Chem. Phys. 110 (1999) 2588.
[44] A.D. Sen, A.K. Shukla, J.H. Futrell, to be published.
[45] Z. Herman, private communication.